J|A|C|S

A R T I C L E S

Chiroptical and Computational Studies of a Bridled Chiroporphyrin and of Its Nickel(II), Copper(II), and Zinc(II) Complexes

Géraldine Maheut,[†,‡] Anna Castaings,[†,‡] Jacques Pécaut,[†]
Latévi Max Lawson Daku,*,[⊥] Gennaro Pescitelli,[§] Lorenzo Di Bari,*,[§] and
Jean-Claude Marchon*,[†]

*Contribution from the Laboratoire de Chimie Inorganique et Biologique, Département de
Recherche Fondamentale sur la Matière Condensée, CEA-Grenoble, 38054 Grenoble, France,
Département Intégration Hétérogène Silicium, Leti, CEA-Grenoble, 38054 Grenoble, France,
Département de Chimie Physique, Université de Genève, 30 quai Ernest Ansermet, CH-1211
Genève 4, Switzerland, and Dipartimento di Chimica e Chimica Industriale, CNR-ICCOM,
Via Risorgimento 35, I-56126 Pisa, Italy*

Received August 31, 2005; E-mail: max.lawson@unige.ch; ldb@dcci.unipi.it; jean-claude.marchon@cea.fr

---

Abstract: Circular dichroism (CD) spectra and density functional theory (DFT) calculations are reported for a series of conformationally bistable chiroporphyrins with 8-methylene bridles MBCP-8, which can display either an $\alpha\alpha\alpha\alpha$ or an $\alpha\beta\alpha\beta$ orientation of their meso substituents. From DFT geometry optimizations, the most stable form of ZnBCP-8 is found to be the $\alpha\alpha\alpha\alpha$ conformer. By passing to NiBCP-8, there is a strong stabilization of the $\alpha\beta\alpha\beta$ conformation with respect to the $\alpha\alpha\alpha\alpha$ conformation, consistent with the X-ray structures of $\alpha\alpha\alpha\alpha$-ZnBCP-8 and $\alpha\beta\alpha\beta$-NiBCP-8. A correlation between the sign of the CD signal in the Soret region and the conformation of the BCP-8 compounds is reported: the $\alpha\alpha\alpha\alpha$ conformers H$_2$BCP-8 and ZnBCP-8 show a positive CD signal, whereas the $\alpha\beta\alpha\beta$ conformers NiBCP-8 and CuBCP-8 exhibit a negative signal. The possible contributions to the rotational strengths of $\alpha\beta\alpha\beta$-NiBCP-8 and $\alpha\alpha\alpha\alpha$-ZnBCP-8, calculated on the basis of their crystal structures, have been analyzed. The CD signals are found to result from a combination of both the inherent chirality of the porphyrin and of extrinsic contributions due to the chiral bridles. These results may have a broad significance for understanding the chiroptical properties of chiral porphyrins and hemoproteins and for monitoring stimuli-responsive, conformationally bistable chiroporphyrin compounds.

Introduction

Notable progress has been made recently in the design of molecular machines and of stimuli-responsive molecules,[1] which conceivably might be used as switch junctions in nanoelectronic devices.[2] Molecular bistability based on an electron- or photon-induced conformation change has attracted considerable interest.[3] In a related area, we have described recently a new family of "bridled" chiroporphyrins, H$_2$BCP-*n*, in which two straps connect adjacent meso substituents by ester linkages, and we

have shown that the length of the strap has a strong influence on the conformation of these molecules.[4]
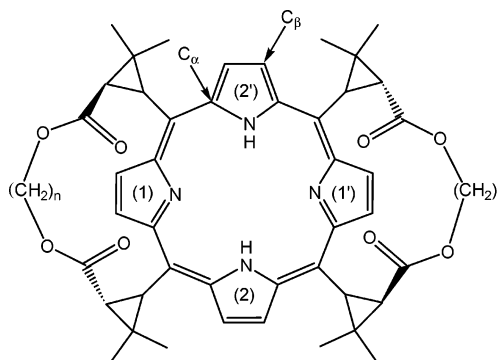
Although long straps with $n = 9-16$ methylene groups favor an $\alpha\beta\alpha\beta$ conformation with alternating up, down meso sub-

---

[†] Département de Recherche Fondamentale sur la Matière Condensée,
CEA-Grenoble.
[‡] Département Intégration Hétérogène Silicium, Leti, CEA-Grenoble.
[⊥] Université de Genève.
[§] CNR-ICCOM.

(1) For recent reviews, see: (a) Feringa, B. L. *Acc Chem. Res.* **2001**, *34*, 504–513. (b) Dietrich-Buchecker, C.; Jimenez-Molero, M. C.; Sartor, V.; Sauvage, J.-P. *Pure Appl. Chem.* **2003**, *75*, 1383–1393. (c) Easton, C. J.; Lincoln, S. F.; Barr, L.; Onagi, H. *Chem.−Eur. J.* **2004**, *10*, 3120–3128. (d) Mandl, C. P.; Konig, B. *Angew. Chem., Int. Ed.* **2004**, *43*, 1622–1624. (e) Kinbara, K.; Aida, T. *Chem. Rev.* **2005**, *105*, 1377–1400. (f) Raymo, F. M.; Tomasulo, M. *Chem. Soc. Rev.* **2005**, *34*, 327–336. (g) Zhang, J.; Albelda, M. T.; Liu, Y.; Canary, J. W. *Chirality* **2005**, *17*, 404–418.
(2) For leading references, see: Raymo, F. M. *Adv. Mater.* **2002**, *14*, 401–414. (b) Kuhr, W. G.; Gallo, A. R.; Manning, R. W.; Rhodine, C. W. *MRS Bulletin* **2004**, *29*, 838–842. (c) Wassel, R. A.; Gorman, C. B. *Angew. Chem., Int. Ed.* **2004**, *43*, 5120–5123. (d) Mendes, P. M.; Flood, A. H.; Stoddart, J. F. *Appl. Phys. A: Mater. Sci. Process.* **2005**, *80*, 1197–1209.

(3) Recent references: (a) Moresco, F.; Meyer, G.; Rieder, K.-H.; Tang, H.; Gourdon, A.; Joachim, C. *Phys. Rev. Lett.* **2001**, *86*, 672–675. (b) Flood, A. H.; Stoddart, J. F.; Steuerman, D. W.; Heath, J. R. *Science* **2004**, *306*, 2055–2056. (c) Qiu, X. H.; Nazin, G. V.; Ho, W. *Phys. Rev. Lett.* **2004**, *93*, 196806. (d) Lastapis, M.; Martin, M.; Riedel, D.; Hellner, L.; Comtet, G.; Dujardin, G. *Science* **2005**, *308*, 1000–1003.

Scheme 1. Bridled Chiroporphyrin Complex as Molecular Nanotweezers[a]
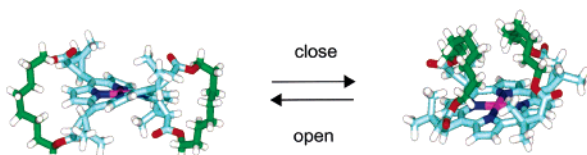
[a](Left) Open Form (X-ray structure of $\alpha\beta\alpha\beta$-NiBCP-8); (Right) Closed Form (X-ray structure of $\alpha\alpha\alpha\alpha$-ZnBCP-8)

stituents, the chiroporphyrin with two 8-methylene bridles H_2-BCP-8 surprisingly exhibits an $\alpha\alpha\alpha\alpha$ conformation in which these substituents are oriented on the same face. Moreover, complexation studies of H_2BCP-8 led to the unexpected discovery that metal insertion can result in a conformation change. Thus, the complex with the large zinc(II) ion ZnBCP-8, like the free base, has an $\alpha\alpha\alpha\alpha$ orientation of the substituents and a nearly planar macrocycle, and the straps on the same face of the porphyrin are folded together like a pair of tweezers (Scheme 1, right).[4] In contrast, the low-spin nickel(II) complex NiBCP-8 displays an $\alpha\beta\alpha\beta$ ruffled conformation of the macrocycle, and the straps wrap around the porphyrin and connect cyclopropyl substituents which are oriented on opposite faces (Scheme 1, left).[5]

We are currently examining the possibility that some metal complexes of H_2BCP-8 could be switched between the two conformations and, thus, behave as molecular nanotweezers. For example, because high-spin nickel(II) is a large ion, similar in size to Zn(II), it is reasonable to expect that high-spin NiBCP-8 could have an $\alpha\alpha\alpha\alpha$ conformation similar to that of ZnBCP-8.[6] In other words, the addition (dissociation) of an axial ligand such as piperidine could close (open) the NiBCP-8 nanotweezers by populating (depopulating) the $d_{x^2-y^2}$ orbital of the Ni center, as shown in Scheme 1. A similar effect might be achieved by photoexcitation (via the Ni (d,d) state) or by one-electron reduction of a suitable metal center (such as Mn(III) in MnClBCP-8, for example).

Preliminary experiments have been carried out using ^{1}H NMR spectroscopy to assess the reality of this supposed conformation change of NiBCP-8 in piperidine solution. Partial conversion to a paramagnetic adduct was obtained by dissolution of NiBCP-8 in neat deuterated piperidine, as judged from the UV–visible spectrum. The 500 MHz ^{1}H NMR of the resulting solution showed a broad peak near 40 ppm at room temperature for the pyrrole protons of the high-spin Ni(II) complex, which is typical of a d_{z^2} $d_{x^2-y^2}$ configuration.[4] This signal is likely a superposition of several unresolved components that are too broad to be detected as separate peaks, and therefore, it has not been possible to determine the signal multiplicity, which could disclose the symmetry of the complex and, hence, its conformation.

Because NMR had proved of little utility, we have investigated other spectroscopic techniques. Given that the bridled chiroporphyrins have four chiral meso substituents derived from (1*R*)-*cis*-hemicaronaldehyde, we have explored their chiroptical

properties in the hope that circular dichroism (CD) would be a good reporter of their conformations.[7,8] We have also performed theoretical calculations to gain a better understanding of the conformations of these switchable complexes. In a first section, density-functional theory (DFT) is used to examine the relative stability of the $\alpha\alpha\alpha\alpha$ and $\alpha\beta\alpha\beta$ conformers for the two ZnBCP-8 and NiBCP-8 complexes, and geometry optimizations are carried out to evaluate the structural and energy differences between the two conformers. In a second section, the CD spectra of the H_2BCP-8 free base and of its nickel(II), copper(II), and zinc(II) complexes are described; those of H_2BCP-9 and of its corresponding complexes are also shown for comparison. We show that there is a simple correlation between the sign of the Cotton effects in the Soret region and the $\alpha\alpha\alpha\alpha$ or $\alpha\beta\alpha\beta$ conformation of these molecules. This correlation allows a facile determination of the solution conformation on the basis of the CD signal. In a third section, we analyze the various possible contributions to the rotational strengths of the nickel and zinc complexes, with a view to understanding the origin of the observed Soret CD. Calculations performed on the basis of the crystal structures indicate that the CD signals result from a combination of both the inherent chirality of the porphyrin and extrinsic contributions due to their chiral environment. These results may have a broad significance toward the understanding of the chiroptical properties of hemoproteins and porphyrin-based compounds, especially in the context of the increasingly popular use of porphyrins as CD reporter groups and structural probes.[7, 8]

Experimental Section

Materials. The synthesis and characterization of the porphyrin free bases H_2BCP-*n* (*n* = 8, 9) have been described in previous papers from our laboratories.[4,5,9] Metal insertion was performed by standard methods.[5] The metal complexes MBCP-*n* (*n* = 8, 9; M = Ni, Cu, Zn) were characterized by UV–visible and NMR spectroscopies and by ES mass spectrometry.

Spectroscopic Methods. CD and UV–visible spectra were recorded with an Applied Photophysics Chirascan spectrometer, a Bio-Logic MOS-450, or a Jasco J-600 using standard conditions (Supporting Information). Porphyrin solutions in dichloromethane were placed in 0.1 cm path quartz cells, and their concentrations were adjusted to obtain an absorbance of ca. 0.8–1.2 unit prior to running the CD spectra. Each spectrum was acquired three times, and the data were averaged. Raw data obtained with the Chirascan and the MOS-450 were smoothed after background subtraction using a Savitsky-Golay algorithm; in every case, the residual was randomly distributed around zero.

Computational Methods. Calculations of conformer structures and energetics were carried out with the Amsterdam Density Functional (ADF) program package,[10,11] using basis sets from the ADF basis set database. ADF uses Slater-type orbital (STO) functions, and to probe the influence of the quality of the basis sets on the results, two sets of STO basis functions S and S' were used. In the S set, a triple-ζ polarized

(4) Gazeau, S.; Pécaut, J.; Marchon, J. C. *Chem. Commun.* **2001**, 1644–1645.

(5) Haddad, R. E.; Gazeau, S.; Pécaut, J.; Marchon, J. C.; Medforth, C. J.; Shelnutt, J. A. *J. Am. Chem. Soc.* **2003**, *125*, 1253–1268.

(6) Song, Y.; Haddad, R. E.; Jia, S.-L.; Hok, S.; Olmstead, M. M.; Nurco, D. J.; Shore, N. E.; Zhang, J.; Ma, J.-G.; Smith, K. M.; Gazeau, S.; Pécaut, J.; Marchon, J. C.; Medforth, C. J.; Shelnutt, J. A. *J. Am. Chem. Soc.* **2005**, *127*, 1179–1192.

(7) (a) Ogoshi, H.; Mizutani, T. *Acc. Chem. Res.* **1998**, *31*, 81–89. (b) Ogoshi, H.; Mizutani, T.; Hayashi, T.; Kuroda, Y. In *The Porphyrin Handbook*; Kadish, K. M., Smith, K. M., Guilard, R., Eds.; Academic Press: San Diego, 2000; Vol. 6, pp 280–340.

(8) (a) Huang, X.; Nakanishi, K.; Berova, N. *Chirality* **2000**, *12*, 237–255. (b) Weiss, J. *J. Inclusion Phenom. Macrocyclic Chem.* **2001**, *40*, 1–22.

(9) Gazeau, S.; Pécaut, J.; Haddad, R.; Shelnutt, J. A.; Marchon, J. C. *Eur. J. Inorg. Chem.* **2002**, 2956–2960.

(10) *Amsterdam Density Functional program*, release ADF2004.01; Theoretical Chemistry, Vrije Universiteit: Amsterdam, The Netherlands, http://www.scm.com.

(11) te Velde, G.; Bickelhaupt, F. M.; Baerends, E. J.; Fonseca Guerra, C.; van Gisbergen, S. J. A.; Snijders, J. G.; Ziegler, T. *J. Comput. Chem.* **2001**, *22*, 931–967.

basis set TZP was used for the Ni and Zn atoms; a double-ζ polarized basis set DZP was employed for the N atoms; and for the O, C, and H atoms, a double-ζ basis set DZ was used. The S' set is similar to the S set except that it includes additional polarization functions for the C and O atoms, which are thus described by DZP basis sets. In the calculations performed with both sets, the core shells were frozen up to the 3p level for Ni and Zn and at the 1s level for C, O, N. The general accuracy parameter "accint" was set to the high value of 4.5, and the other program parameters were kept to their default values. Calculations were run restricted for the zinc(II) and nickel(II) complexes. In all cases, the symmetry of the complexes was constrained to C_2. Note that the C_2 symmetry operation interchanges opposite pyrrole rings and that one, therefore, verifies for the metal–nitrogen distances: $M-N_i = M-N_{i'}$; with $M = Zn$, Ni and $i = 1, 2$.

Semiempirical (ZINDO formulation) and time-dependent DFT (BH&HLYP functional, TZVP basis) calculations were performed on the excited states of porphyrin rings of ZnBCP-8 and NiBCP-8, both of C_1 (solid-state) and axially symmetric (C_2 and D_2, respectively) structures. ZINDO and TDDFT calculations were run with Gaussian 03 (revision B.05).[12,13] The two coupling mechanisms for ZnBCP-8 and NiBCP-8 were estimated with eqs 4 and 8, shown below (section III.C–D). Geometrical factors were taken from solid-state structures and spectroscopic factors for the Soret band from experimental absorption spectra. The frequency separation between the two Soret components was put equal to that found by TDDFT calculations on the porphyrin cores. Soret transitions were considered polarized along N–N directions, $n-\pi^*$ along C=O, and $\pi-\pi^*$ along the direction defined by carbonyl O and the middle of C–O single bond, in keeping with ZINDO calculations on methyl acetate.

Results and Discussion

I. Structures and Energetics of ZnBCP-8 and NiBCP-8.
The energy difference ΔE_{cnf} between the two conformers reads

$$\Delta E_{cnf} = E_{min}(\alpha\beta\alpha\beta) - E_{min}(\alpha\alpha\alpha\alpha) \tag{1}$$

where $E_{min}(\alpha\alpha\alpha\alpha)$ and $E_{min}(\alpha\beta\alpha\beta)$ represent the minimized energies of the $\alpha\alpha\alpha\alpha$ and $\alpha\beta\alpha\beta$ conformers, respectively. It follows from the convention used for ΔE_{cnf} that the $\alpha\alpha\alpha\alpha$ conformation is the most stable one for $\Delta E_{cnf} > 0$.

Quantum chemical methods are expected to give a quantitatively accurate description of the geometry and energetics of the BCP-8 complexes, which should help achieve a thorough understanding of their stereochemistry. Although the use of computationally demanding high-level ab initio (i.e., wave function-based) methods is precluded by the large number of atoms (145) present in these systems, DFT methods can efficiently be applied to systems of such size. In particular, the ability of most approximate exchange–correlation density functionals that go beyond the local density approximation (LDA) to accurately describe the geometry and energetics of molecular systems is well established.[14] The LDA tends to overestimate bond energies. The generalized gradient approximation (GGA) remedies this deficiency by adding correction terms that depend on the density gradient and allow a better

description of exchange and correlation. The GGA improves the LDA description of equilibrium geometries and energetics, and most GGA functionals are likely to deliver satisfactory results for the energetics and geometries of the conformers. However, the recent PBE GGA offers the avantage over other GGAs that it has been derived from first-principle arguments and, thus, obeys many physical constraints that are not necessarily obeyed by other functionals.[15] We therefore used the PBE functional for the study of the ZnBCP-8 and NiBCP-8.

The calculations led to the characterization of the closed-shell Zn(II) and low-spin Ni(II) chiroporphyrin complexes in their electronic ground state of ^1A symmetry. For both complexes, the optimized structures of their $\alpha\alpha\alpha\alpha$ and $\alpha\beta\alpha\beta$ conformers respectively exhibit a doming and a ruffling of the porphyrin macrocycle, as observed in the X-ray structures of $\alpha\alpha\alpha\alpha$-ZnBCP-8 and $\alpha\beta\alpha\beta$-NiBCP-8 shown in Scheme 1. Important structural parameters for characterizing the geometries of the BCP-8 complexes in the $\alpha\alpha\alpha\alpha$ and $\alpha\beta\alpha\beta$ conformations are (i) the average metal–nitrogen bond length, which gives a measure of the contraction of the porphinato core;[16] (ii) the displacement of the metal atom out of the mean plane of the 24 atoms of the porphyrin core M–Ct (M = Zn, Ni; Ct = the projection of the metal atom on the mean plane); (iii) the root-mean-square (RMS) out-of-plane displacement Δ_{RMS}, which provides a measure of the deviation of the porphyrin macrocycle from planarity and which is given by:[17]

$$\Delta_{RMS} = \sqrt{\frac{1}{24}\sum_{k=1}^{24}\delta_k^2} \tag{2}$$

where δ_k is the orthogonal displacement of the k-th atom of the macrocycle from the mean plane; (iv) and the average torsional angle $C_\alpha-N-N-C_\alpha$ between opposite pyrrole rings, which gives a measure of the ruffling of the porphyrin and which is also known as the ruffling angle.[6,17] The values of these parameters are given in Table 1 for the optimized and available experimental geometries of ZnBCP-8 and NiBCP-8.

Inspection of Table 1 shows that the quality of the basis sets used has a limited influence on the theoretical values found for the key structural parameters. Thus, passing from the S set to the larger S' set essentially translates into a ~0.01 Å decrease of the optimized metal–nitrogen distances for the conformers of the two complexes. One also notes that there is a good agreement between the experimental and theoretical parameter values found for the $\alpha\alpha\alpha\alpha$ conformer of ZnBCP-8 and for the $\alpha\beta\alpha\beta$ conformer of NiBCP-8. For instance, the optimized structures of $\alpha\alpha\alpha\alpha$-ZnBCP-8 and $\alpha\beta\alpha\beta$-NiBCP-8 exhibit metal–nitrogen distances that are slightly longer than those experimentally observed. In fact, given that our calculations are performed for the two complexes in the gas phase and, thus, do not take into account crystal packing forces, there is no reason to expect that the experimental and optimized geometries should strictly match. Crystal packing forces are indeed known to have considerable influences on the geometries and conformations of porphyrin complexes,[17] and they are responsible for the

(12) Frisch M. J.; et al. *Gaussian 03*, revision B.05; Gaussian, Inc.: Pittsburgh, PA, 2003. For a description of calculations methods see program documentation at http://www.Gaussian.com/g_ur/g03mantop.htm.

(13) For a few recent examples of semiempirical and TDDFT calculations on distorted porphyrins see ref 5 and: (a) Ryeng, H.; Ghosh, A. *J. Am. Chem. Soc.* **2002**, *124*, 8099–8103. (b) Prabhu, N. V.; Dalosto, S. D.; Sharp, K. A.; Wright, W. W.; Vanderkooi, J. M. *J. Phys. Chem. B* **2002**, *106*, 5561–5571. (c) Di Magno, S. G.; Wertsching, A. K.; Ross, C. R., II. *J. Am. Chem. Soc.* **1995**, *117*, 8279–80.

(14) Koch, W.; Holthausen, M. C. *A Chemist's Guide to Density Functional Theory*; Wiley-VCH: New York, 2000.

(15) Perdew, J. P.; Burke, K.; Ernzerhof, M. *Phys. Rev. Lett.* **1996**, *77*, 3865–3868; Erratum: *Phys. Rev. Lett.* **1997**, *78*, 1396.

(16) Scheidt, W. R.; Reed, C. A. *Chem. Rev.* **1981**, *81*, 543–555.

(17) Jentzen, W.; Turowska-Tyrk, I.; Scheidt, W. R.; Shelnutt, J. A. *Inorg. Chem.* **1996**, *35*, 3559–3567.

Table 1. Selected Structural Parameters in the Optimized Geometries of ZnBCP-8 and NiBCP-8

porphyrin	theoretical level	M–N₁ (Å)	M–N₂ (Å)	M–Nᵃ (Å)	M–Ct (Å)	Δ_RMS (Å)	Cₐ–N–N–Cₐ (deg)
αααα-ZnBCP-8	PBE/S	2.091	2.077	2.084	0.246	0.155	3.1
	PBE/S′	2.081	2.067	2.074	0.238	0.153	3.2
αβαβ-ZnBCP-8	PBE/S	2.063	2.073	2.068	0.000	0.179	17.7
	PBE/S′	2.052	2.062	2.057	0.003	0.188	18.7
αααα-ZnBCP-8ᵇ	-	2.046, 2.027	2.045, 2.046	2.041	0.147	0.128	3.1
	-	2.034, 2.031	2.029, 2.025	2.030	0.111	0.117	4.3
αααα-NiBCP-8	PBE/S	2.004	1.981	1.993	0.185	0.129	5.4
	PBE/S′	1.994	1.972	1.983	0.175	0.126	5.7
αβαβ-NiBCP-8	PBE/S	1.944	1.953	1.949	0.027	0.351	36.0
	PBE/S′	1.934	1.945	1.940	0.022	0.353	36.3
αβαβ-NiBCP-8ᵇ	-	1.921, 1.925	1.901, 1.915	1.916	0.006	0.373	38.1
	-	1.921, 1.921	1.909, 1.917	1.917	0.014	0.386	37.6

ᵃ Average M−N distance. ᵇ Structural parameter values for the two independent (ZnBCP-8 or NiBCP-8) molecules present in the crystal.[4] The two values given for M−Nᵢ correspond to the M−Nᵢ and M−Nᵢ′ distances, (i = 1, 2), which are not necessarily equal because of the lack of symmetry of the molecules in the crystal.

coexistence of two distinct, albeit similar, molecular structures in the studied crystals of αααα-ZnBCP-8 and αβαβ-NiBCP-8.[4,5] Therefore we consider that the agreement between the theoretical and experimental parameter values reported for αααα-ZnBCP-8 and αβαβ-NiBCP-8 is very satisfactory, and that it is indicative of a close similarity between the optimized and the X-ray structures.

Upon the αααα → αβαβ isomerization, the optimized M−N bonds undergo shortenings that average to 0.02 Å for ZnBCP-8 and to 0.04 Å for NiBCP-8. These decreases in the metal−nitrogen distances compare well with the decrease of the M−N bond lengths of 0.02−0.03 Å observed in porphyrin complexes upon ruffling of the porphyrin macrocycle.[16] For the two complexes, the αααα → αβαβ change of conformations and the concomitant ruffling of the macrocycle translate in Table 1 into the reduction of the out-of-plane metal atom displacement, a large increase of the RMS out-of-plane displacement, and an increase of the ruffling angle by a factor of about 6−7. The large ruffling of the porphyrin core actually allows the macrocycle to accommodate the alternating up, down meso substituents; it may also be influenced by the constraints imposed by the short straps that link the adjacent meso substituents that are located on opposite faces of the macrocycle.[4] Interestingly, our calculations predict for the isolated BCP-8 complexes that the shortening of the M−N distances upon the αααα → αβαβ change of conformations principally affects the M−N₁ distances, that is, the lengths of the bonds linking the metal center to the pyrroles caught in the bridles. This supports the idea that the constraints imposed by the bridles may play a key role in the ruffling of the porphyrin core of bridled chiroporphyrins.[4,9]

For a given conformation of the bridled chiroporphyrin, one notes in Table 1 that the metal−nitrogen bonds undergo upon the Zn(II) → Ni(II) substitution a shortening of ~0.1 Å, which is due to the fact that the antibonding level of $d_{x^2-y^2}$ type,[18] which is filled in the d^{10} Zn(II) complex, becomes unoccupied in the low-spin d^8 Ni(II) complex. The noticeable increase of the ruffling angle by ~2 degrees shows that the contraction of the porphyrin core in the αααα conformation upon the Zn(II) → Ni(II) substitution induces or enhances the out-of-plane

(18) We refer to the metallic molecular orbitals using denominations such as "antibonding $d_{x^2-y^2}$- or d_{z^2}-type orbital" for the antibonding σ-type orbitals involving the metallic 3d atomic orbitals of octahedral e_g parentage. The resulting simplified orbital picture provides a convenient, physically meaningful tool for discussing the properties of the porphyrin complexes, in particular, their stereochemistry.[16]

Table 2. Calculated Values of the Energy Difference ΔE_cnf for ZnBCP-8 and NiBCP-8

	ΔE_cnf (cm⁻¹)	
theoretical level	ZnBCP-8	NiBCP-8
PBE/S	+2449	+453
PBE/S′	+2769	+843

distortion of the macrocycle along the ruffling distortion mode.[5] This is more obvious when one considers the results obtained for the complexes in the αβαβ conformation because one observes in this case that the RMS out-of-plane displacement and the ruffling angle drastically increase.

The calculated values of the energy difference ΔE_cnf between the αααα and αβαβ conformers of the BCP-8 complexes are given in Table 2. These quantities are all positive, and the αααα conformation is therefore predicted to be the most stable conformation for the two complexes.

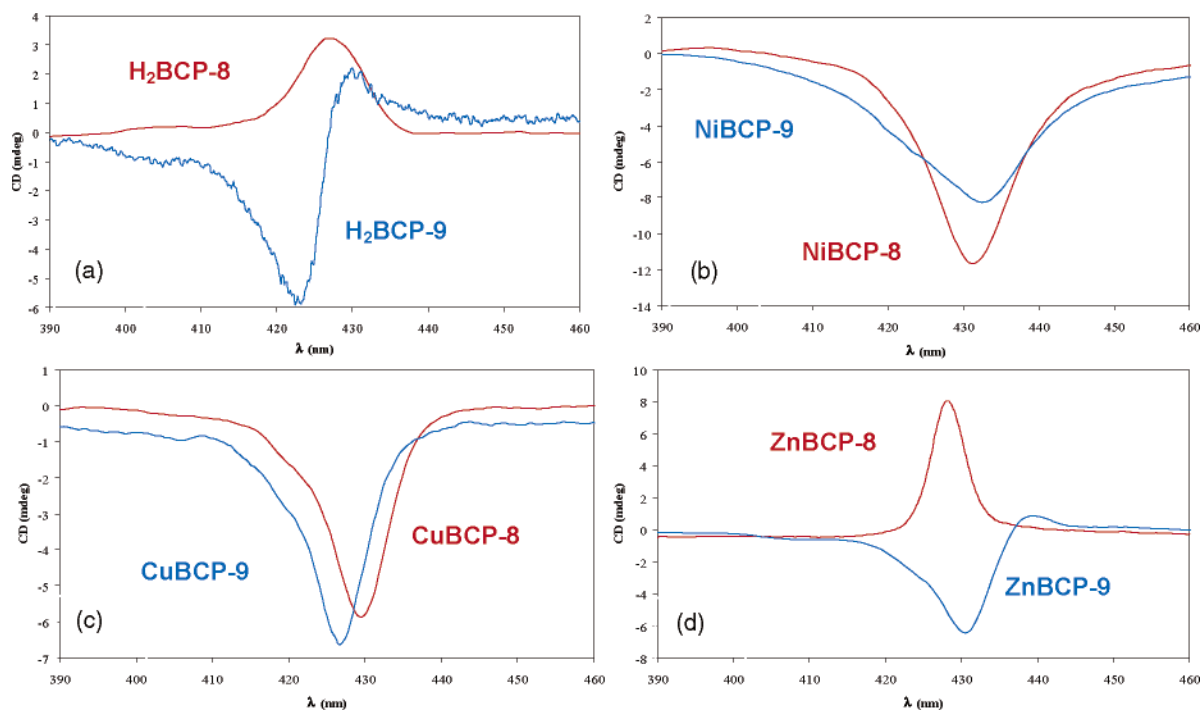For the Zn(II) complex, which is obtained and isolated in the αααα conformation,[4] our results are in agreement with experiment. We note, however, that whereas for ZnBCP-8 the energy difference ΔE_cnf takes a value of 2449 cm⁻¹ for the calculations performed at the PBE/S level, it drastically drops on passing to NiBCP-8, taking a value of 453 cm⁻¹. This shows that the αααα conformation is energetically strongly favored by the long metal−nitrogen bonds found in the Zn(II) complex, and that the large shortening undergone by these bonds when passing to the LS Ni(II) complex substantially stabilizes the αβαβ conformation, bringing the two conformations close in energy, consistent with the observed stereochemistry of the two complexes.

Consequently, the discrepancy between the outcome of the conformational analysis and the experiment can tentatively be ascribed to the neglect of the environmental effects as this constitutes the last major approximation in our study performed for the complexes in the gas phase. Noticing that the αααα and αβαβ conformers of ZnBCP-8 and NiBCP-8 have very different dipole moments (the dipole moment of each complex is consistently found to be smaller in the αβαβ conformation than in the αααα conformation, see Table 3), and keeping in mind that the synthesis of the complexes takes place in solution, solvent effects turn out to be the environmental effects that should be considered first. An implicit solvation model such as the conductorlike screening model is well suited for accounting

Table 3. Dipole Moments (debye) of ααα α and αβα β Conformers of ZnBCP-8 and NiBCP-8

theoretical level	ααα α-ZnBCP-8	αβα β-ZnBCP-8	ααα α-NiBCP-8	αβα β-NiBCP-8
PBE/S	1.09	0.02	1.48	0.18
PBE/S'	1.42	0.00	1.82	0.17

Figure 1. CD spectra in CH_2Cl_2 for the Soret transitions of (a) H_2BCP-*n*, (b) NiBCP-*n*, (c) CuBCP-*n*, and (d) ZnBCP-*n*. Red: *n* = 8; blue: *n* = 9.

for the solvent effects in an elaborated manner.[19] This, however, is beyond the scope of the present study.

II. Experimental CD Spectra. The CD spectra obtained in the Soret region are illustrated in Figure 1 for the free-base porphyrins H_2BCP-*n* (*n* = 8−9) and their square-planar nickel-(II), copper(II), and zinc(II) complexes MBCP-*n* (M = Ni, Cu, Zn; *n* = 8−9). The CD spectrum of the porphyrin free-base H_2BCP-8, which has an ααα α conformation,[4] displays a positive Cotton effect in the Soret band region. In contrast, the CD spectrum of H_2BCP-9, which has a αβα β conformation,[4,5,9] shows a negative Cotton effect in this region (Figure 1a), with a small positive long-wavelength lobe. Similarly for the zinc complexes, a positive Cotton effect is observed for ααα α-ZnBCP-8,[4] and a negative Cotton effect (unsymmetrical, with a weak long-wavelength positive component) is seen for αβα β-ZnBCP-9 (Figure 1d).[4,5,9] The αβα β nickel complexes NiBCP-8 and NiBCP-9 [5] both display an intense negative Cotton effect in the Soret region (Figure 1b). Thus, the main feature of the CD spectrum seems to be correlated to the molecular conformation in this series: the αβα β conformation gives rise to a negative Cotton effect, independent of the central metal and of the bridle length, while the ααα α conformation gives rise to a positive Cotton effect. This observation also leads to the safe conclusion that the copper(II) complexes CuBCP-*n* (*n* = 8−9), which display an intense negative Cotton effect (Figure 1c), both have an αβα β conformation.

III. Contributions to the Soret CD of ZnBCP-8 and NiBCP-8. A. Analysis. Electronic CD is observed in cor-

respondence with electronic transitions endowed with nonnegligible rotational strength:[20]

$$R_i = \mathrm{Im}(\mu_{0i} \cdot \mathbf{m}_{i0}) \qquad (3)$$

where μ_{0i} and $\mathbf{m}_{i0}$ (respectively, the electric and magnetic transition dipoles associated to the $0 \rightarrow i$ transition) are measures of the linear and circular displacements of charge upon excitation. In the context of electronic spectroscopies, a common approach consists of identifying chromophoric groups to which observed transitions are mostly confined. If the chromophore is chiral, the combination of μ_{0i} and $\mathbf{m}_{i0}$ results in a helical displacement of charge, which interacts differently with left- and right-circularly polarized light, generating an intrinsic rotational strength. Because most chromophores, like planar porphyrins and carboxyl groups, are inherently achiral, their electronic transitions have pure electric dipole-allowed or magnetic dipole-allowed character, or the μ and $\mathbf{m}$ dipoles are orthogonal. In such cases, optical activity may be thought to arise from various mechanisms allowing for different transitions to mix and gain nonorthogonal and nonvanishing electric and magnetic transition dipoles. The resulting rotational strength can be approximated [21] as the sum of three contributions:

(1) the coupled-dipole, or $\mu \cdot \mu$ coupling, or exciton mechanism: the chromophore undergoes an electric dipole-allowed

(19) Pye, C. C.; Ziegler, T. *Theor. Chem. Acc.* **1999**, *101*, 396−408.

(20) (a) Mason, S. F. *Molecular Optical Activity and the Chiral Discrimination*; Cambridge University Press: Cambridge, 1982. (b) Rodger, A.; Nordén, B. *Circular Dichroism & Linear Dichroism*; Oxford University Press: Oxford, 1997. (c) *Circular Dichroism: Principles and Applications*, 2nd ed.; Berova, N., Nakanishi, K., Woody, R. W., Eds.; Wiley-VCH: New York, 2000.

(21) Tinoco, I., Jr. *Adv. Chem. Phys.* **1962**, *4*, 113−160.

Scheme 2. Calculated Deviations of the Heavy Atoms upon Symmetrization of the Porphyrin Cores
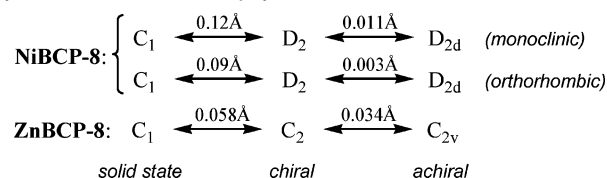
transition that couples with other electric dipole-allowed transitions elsewhere in the molecule, thus generating magnetic dipoles too;

(2) the dynamic or $\mu \cdot m$ coupling mechanism: the chromophore undergoes an electric dipole-allowed transition that couples with a magnetic dipole-allowed transition elsewhere in the molecule (or vice-versa);

(3) the static coupling or one-electron mechanism: different electric and magnetic dipole-allowed transitions on the chromophore are allowed to mix due to perturbation exerted by the chiral environment.

Inspection of the structures of the bridled metalloporphyrins suggests that all four mechanisms (intrinsic chirality plus 1−3) may contribute to the observed chiroptical properties. The first three have been evaluated quantitatively, and in the following, we examine them in detail with reference to the compounds ZnBCP-8 and NiBCP-8, whose solid-state structures are available, taken as paradigms of the two $\alpha\alpha\alpha\alpha$ and $\alpha\beta\alpha\beta$ classes.

B. The Inherent Chirality. The only way of estimating the contribution of inherent chirality lies in quantum mechanical calculations.[22] The porphyrin cores in both solid-state structures[4] are devoid of any symmetry element; they present nonplanar distortions of the ruffling ($\alpha\beta\alpha\beta$-NiBCP-8) and doming ($\alpha\alpha\alpha\alpha$-ZnBCP-8) type.[5,24] In solution, NMR demonstrates that Zn-BCP-8 and NiBCP-8 display average C_2 and D_2 symmetry, respectively, suggesting that the porphyrin rings themselves are at least C_2 and D_2 symmetric for spectra averaged over a sufficiently long time. Starting from the published X-ray structures,[4] symmetric porphyrin cores were generated by removing the bridles, adding meso hydrogens, and optimizing the porphyrin cores with the minimal restraints imposing the desired symmetry. In the case of NiBCP-8, four independent structures are available,[5] and calculations were run both for the most distorted (monoclinic, molecule A; total nonplanar distortion[24] d_{tot} = 1.962 Å, ruffling deformation d_{ruf} = 1.893 Å) and the least distorted structure (orthorhombic, molecule A; d_{tot} = 1.827 Å, d_{ruf} = 1.778 Å). We also noticed that calculated chiral cores are not far from achiral structures such as C_{2v} for ZnBCP-8 and D_{2d} for NiBCP-8, as shown by the calculated RMS deviations for the porphyrin heavy atoms (C, N, metal) shown in Scheme 2.

Semiempirical and time-dependent DFT calculations were thus performed on the excited states of porphyrin rings of ZnBCP-8 and NiBCP-8, both of C_1 (solid-state) and axially symmetric (C_2 and D_2, respectively) structures.[22,23]

C. The $\mu \cdot \mu$ Mechanism. Other possible mechanisms of optical activity arising from the coupling of Soret transitions with extrachromophoric groups were also considered. The four ester groups in ZnBCP-8 and NiBCP-8 may provide effective coupling terms of both electric dipole-allowed ($\pi-\pi^*$ transition, around 170 nm) and magnetic dipole-allowed ($n-\pi^*$ transition, around 210 nm) types. The coupled dipoles or exciton mechanism of optical activity is the most investigated one.[20,25] It arises whenever two electric dipole allowed transitions are sufficiently close in energy and their transition dipoles are arranged in a dissymmetric way (not collinear or coplanar or related by roto-reflection elements of symmetry). The rotational strengths allied to such transitions are opposite in sign and of the same intensity (the so-called CD couplet) and may be quantitatively predicted through the equation:[20a,b,25a]

$$R_{12} = \pm \frac{2\pi\nu_1\nu_2}{\nu_2^2 - \nu_1^2} V_{12} \mathbf{R}_{12} \cdot \mu_1 \times \mu_2 \qquad (4)$$

where ν_1 and ν_2 are the transition frequencies (or wavenumbers), μ_1 and μ_2 are the transition dipole vectors, $\mathbf{R}_{12}$ is their distance vector (with modulus R_{12}), and V_{12} is their coupling potential, which is usually approximated as the dipole−dipole term:

$$V_{12} = \frac{\mu_1 \cdot \mu_2}{R_{12}^3} - \frac{3(\mu_1 \cdot \mathbf{R}_{12})(\mu_2 \cdot \mathbf{R}_{12})}{R_{12}^5} \qquad (5)$$

The popularity of the exciton mechanism lies in the fact that eq 4 leads to a simple and immediate correlation between the molecular structure and the sign of the CD spectrum: when the two dipoles define a positive chirality, i.e., the dipole in the front must be rotated clockwise to be superimposed to that in the back, the resulting CD couplet is positive, that is, its long-wavelength component is positive, and vice-versa.[25] Because Soret transitions have a strong transition dipole, the exciton method has been extensively applied to porphyrin-containing compounds,[26] and especially bis-porphyrins.[27] In particular, the coupling with ester $\pi-\pi^*$ transition has been considered too.[28] In this study, the rotational strength arising from the $\mu \cdot \mu$ coupling for ZnBCP-8 and NiBCP-8 was estimated using eq 4 (see Computational Methods above).

D. The $\mu \cdot m$ Mechanism. The electric-magnetic coupling or $\mu \cdot m$ mechanism[20] has been treated with special reference to the carbonyl chromophore.[29] The rotational strength allied to a magnetic dipole allowed transition (at energy E_m, directed along z axis) coupled to an electric dipole-allowed one (at energy E_μ, with nonnegligible z-component) is:

(22) Cramer, J. C. *Essentials of Computational Chemistry*; Wiley: Chichester, 2002.
(23) In the case of C_2-symmetric Zn porphyrin, Soret transition dipole directions are not symmetry determined; in fact, ZINDO and TDDFT results predict transition dipoles along the $C_{meso}-C_{meso}$ direction. Calculations in Figure 2d,f, bottom, repeated with such orientation led to equivalent results (same signs and discrepancies in intensity within 10%). See Computational Methods.
(24) Shelnutt, J. A.; Song, X.-Z.; Ma, J.-G.; Jia, S.-L.; Jentzen, W.; Medforth, C. J. *Chem. Soc. Rev.* **1998**, *27*, 31−41.

(25) (a) Harada, N.; Nakanishi, K. *Circular Dichroic Spectroscopy−Exciton Coupling in Organic Stereochemistry*; University Science Books: Mill Valley, CA, 1983. (b) Berova, N.; Nakanishi, K. In *Circular Dichroism: Principles and Applications*, 2nd ed.; Berova, N., Nakanishi, K., Woody, R. W., Eds.; Wiley-VCH: New York, 2000; pp 337−382.
(26) For example: (a) Mizutani, T.; Ema, T.; Yoshida, T.; Kuroda, Y.; Ogoshi, H. *Inorg. Chem.* **1993**, *32*, 2072−2077. (b) Di Bari, L.; Pescitelli, G.; Reginato, G.; Salvadori, P. *Chirality* **2001**, *13*, 548−555.
(27) (a) Matile, S.; Berova, N.; Nakanishi, K.; Fleischhauer, J.; Woody, R. W. *J. Am. Chem. Soc.* **1996**, *118*, 5198−5206. (b) Pescitelli, G.; Gabriel, S.; Wang, Y.; Fleischhauer, J.; Woody, R. W.; Berova, N. *J. Am. Chem. Soc.* **2003**, *125*, 7613−7628.
(28) Mizutani, T.; Ema, T.; Yoshida, T.; Renne, T.; Ogoshi, H. *Inorg. Chem.* **1994**, *33*, 3558−3566.

$$R_m = i\mu^z m^z \frac{2E_\mu}{E_\mu^2 - E_m^2} V \tag{6}$$

where V, the coupling potential, is approximated by that between the electric dipole and the electric quadrupole associated with the magnetic dipole:

$$V_{\mu Q} = \frac{\mathbf{R}_{12} \cdot \mathbf{Q} \cdot \mu}{R_{12}^5} - \frac{5}{2} \frac{(\mathbf{R}_{12} \cdot \mathbf{Q} \cdot \mathbf{R}_{12})(\mathbf{R}_{12} \cdot \mu)}{R_{12}^7} \tag{7}$$

The rotational strength allied to the electric dipole-allowed transition is, of course, $R_\mu = -R_m$. For a carbonyl chromophore lying in the yz plane with C—O centered in the origin and directed along z, the quadrupole tensor $\mathbf{Q}$ reduces to its xy off-diagonal terms Q^{xy}, and eq 6 takes the form:[29]

$$R_m = \frac{6E_\mu}{E_\mu^2 - E_m^2} \frac{im^z Q^{xy}}{R_{12}^7}[(R_{12}^2 - 5X^2)Y\mu^x +$$
$$(R_{12}^2 - 5Y^2)X\mu^y - 5XYZ\mu^z]\mu^z \tag{8}$$

where (X,Y,Z) is the dipole position in the above framework and μ^x, μ^y, and μ^z are its components. In eq 8, the factor $im^z Q^{xy}$ is not easily accessible, so it is assessed in an empirical way; for carbonyl $n-\pi^*$ transition, it amounts to 1.89×10^{-46} cgs units.[29a] In this study, we have approximated the ester group by a carbonyl, on the basis of the observation that the $n-\pi^*$ transition is very similar for the two groups (located on and with magnetic dipole directed along C=O, from ZINDO calculations on methyl acetate). Equation 8 was applied to estimate the rotational strength arising from the $\mu \cdot$m coupling for ZnBCP-8 and NiBCP-8 (see Computational Methods above).

E. Intrinsic Rotational Strength. Inherently chiral porphyrins are of high interest, because many heme-containing proteins present distorted porphyrin rings where the distortion plays a crucial biological role.[24,30] Recently, the inherent chirality mechanism has been examined in the case of carbonmonoxy myoglobin,[31] for which deviations from planarity introduce chirality in the heme. It has been demonstrated that the rotational strengths for the two Soret transitions are opposite in sign and their absolute intensities are similar and directly proportional to the degree of ruffling of the heme and may reach very large values (up to 2 DBM, i.e., 2×10^{-38} cgs). However, because the two Soret components are very close in energy, the two CD bands cancel each other to a large extent and moderate net effects result.[31]

In the present case, the axially symmetric distribution of chiral meso substituents in NiBCP-8 and ZnBCP-8 generates nonplanar distortions which make their porphyrin cores inherently chiral. The two Soret or B transitions[32] of each porphyrin are usually very close in energy but generally not degenerate, and they may be associated with moderate to strong rotational strengths. The

(29) (a) Höhn, E. G.; Weigang, O. E., Jr. *J. Chem. Phys.* **1968**, *48*, 1127–1137. (b) Schellman, J. A. *Acc. Chem. Res.* **1968**, *1*, 144–151. (c) Woody, R. W.; Tinoco, I., Jr. *J. Chem. Phys.* **1967**, *46*, 4927–4945.
(30) Ravikanth, M.; Chandrasekhar, T. K. *Struct. Bonding* **1995**, *82*, 105–188.
(31) Kiefl, C.; Sreerama, N.; Haddad, R.; Sun, L.; Jentzen, W.; Lu, Y.; Qiu, Y.; Shelnutt, J. A.; Woody, R. W. *J. Am. Chem. Soc.* **2002**, *124*, 3385–3394.
(32) (a) Ghosh, A. In *The Porphyrin Handbook*; Kadish, K. M., Smith, K. M., Guilard, R., Eds.; Academic Press: San Diego, 2000; Vol. 7, pp 1–38. (b) Gouterman, M. In *The Porphyrins*; Dolphin, D., Ed.; Academic Press: New York, 1978; Vol. III, pp 1–165.

Table 4. Computed Soret Transition Wavelengths and Rotational Strengths[a] of NiBCP-8 and ZnBCP-8 for X-ray Derived and Axially Symmetric DFT-Optimized Structures

	NiBCP-8[b]							
	ZINDO				TDDFT			
	X-ray		D_2		X-ray		D_2	
	λ (nm)	R	λ (nm)	R	λ (nm)	R	λ (nm)	R
B1	399.5	−125	376.2	−123	337.7	−622	336.0	−571
B2	393.3	+160	375.7	+130	335.6	+615	335.8	+589

	ZnBCP-8							
	ZINDO				TDDFT			
	X-ray		C_2		X-ray		C_2	
	λ (nm)	R	λ (nm)	R	λ (nm)	R	λ (nm)	R
B1	384.5	−22	368.6	+6.7	332.9	+2.4	334.3	+8.4
B2	384.0	+18	368.5	+1.7	332.9	−1.2	334.1	+6.6

[a] R in 10^{-40} cgs units. [b] Data shown for NiBCP-8 obtained for the most distorted monoclinic A molecule.[5] R values obtained for the least distorted orthorhombic A molecule[5] are slightly smaller: ZINDO: X-ray: −107/+112; D_2: −118/+120. TDDFT: X-ray: −380/+382; D_2: −563/+570.

ruffled Ni—porphyrin is expected to exhibit stronger intrinsic effects than the moderately domed Zn—porphyrin.

Results for ZINDO and TDDFT calculations of Soret transitions are shown in Table 4. The ruffled Ni—porphyrin exhibits strong rotational strengths of opposite sign for the two Soret components; absolute ZINDO values are in keeping with those calculated for myoglobin with a similar semiempirical method,[31] while TDDFT values are about five times larger.

When a bandwidth (Gaussian shape with 750 cm^{-1} half-height width) is assigned to the computed transitions (Figure 2a), it becomes apparent that mutual cancellation between the two opposite CD bands is extensive and the resulting CD is of moderate intensity. Absolute rotational strengths for the two B transitions of the domed Zn—porphyrin are 2 orders of magnitude smaller, but of the same sign for the C_2-symmetric structure, which gives rise to overall positive CD only two times weaker than for the Ni—porphyrin (Figure 2b). The overestimation of all the computed transition frequencies with respect to experimental spectra (especially evident for TDDFT) is a common fault of electronic excited-state calculations,[22] which does not invalidate other computed quantities such as the sign and relative intensity of rotational strengths.
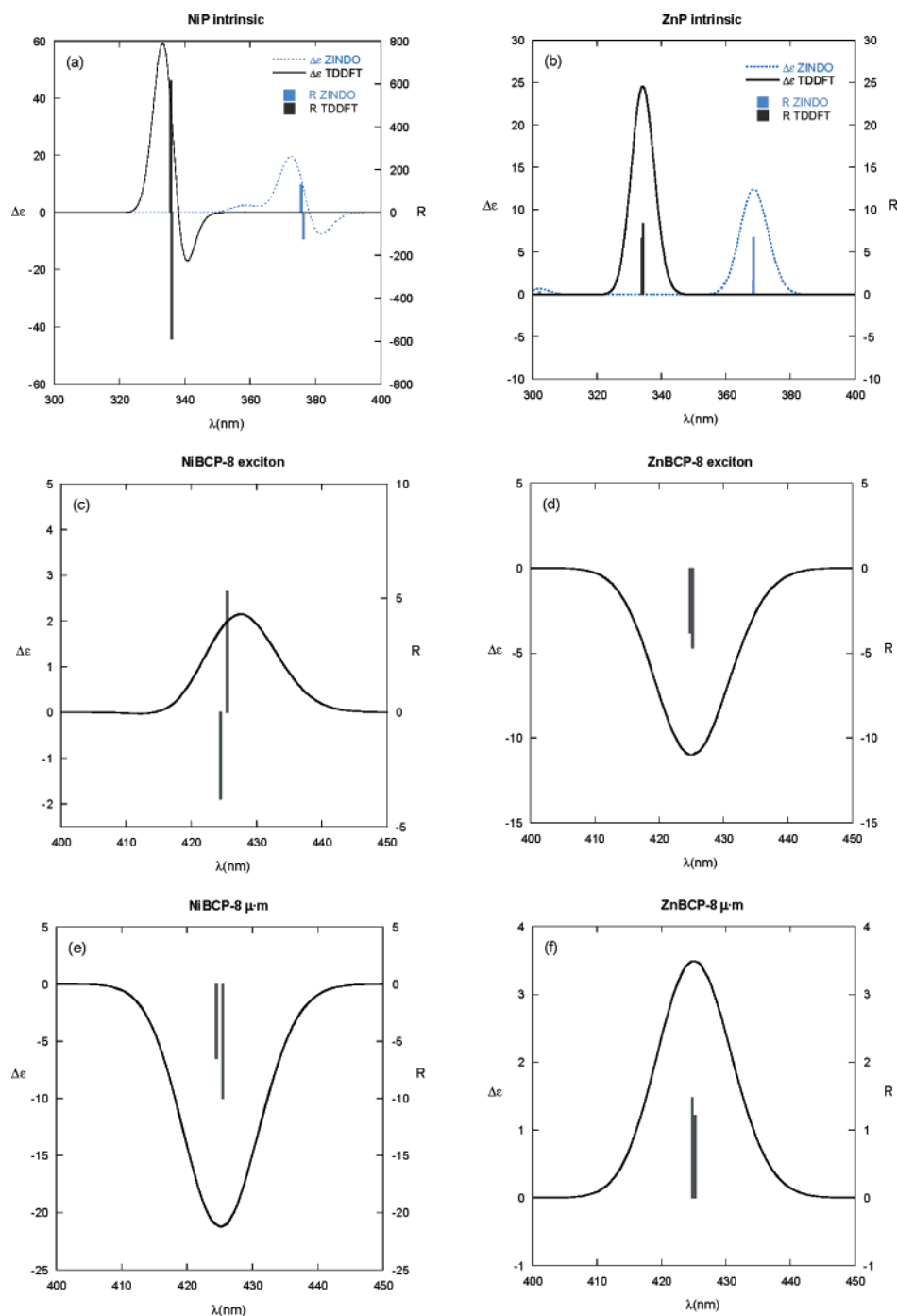
F. Extrinsic Rotational Strength. A case quite similar to the present one has been discussed by Mizutani et al.,[28] concerning the coupling between the Soret transitions of a Zn—porphyrin and $\pi-\pi^*$ and $n-\pi^*$ transitions of an amino acid bound to Zn via the amino group; in that case, the carbonyl plane lies above the porphyrin plane and is almost parallel to it. Explicit semiempirical quantum mechanical calculations led to rotational strengths up to 5×10^{-40} cgs for the coupled dipoles Soret/C=O$_{\pi-\pi^*}$ coupling and up to five times weaker for the $\mu \cdot$m Soret/C=O$_{n-\pi^*}$ coupling.[28] The sign and magnitude depended on the relative orientation between the carbonyl and porphyrin, and the contributions for the two nondegenerate Soret components were opposite for many (but not all) of the orientations considered. The results of our calculations for NiBCP-8 and ZnBCP-8 are summarized in Figure 2c–f, which show overall rotational strengths (sum over four carbonyl groups) and CD spectra computed after application of a Gaussian bandwidth. For both compounds, the coupled dipole mechanism

Figure 2. Computed rotational strengths (vertical bars) and CD spectra (as sum of Gaussians) of Soret transitions for NiBCP-8 and ZnBCP-8 for the three mechanisms: (a,b) intrinsic (from TDDFT and ZINDO calculations on axially symmetric DFT-optimized structures); (c,d) exciton coupling with esters (from X-ray structures and eq 4); (e,f) μ·m coupling with esters (from X-ray structures and eq 8).

generates an overall Soret CD band of opposite sign to the μ·m one; in the case of NiBCP-8, the magnetic coupling overcomes the electric one, while the opposite is true for ZnBCP-8. Given the roughly symmetric properties of the two complexes, the four carbonyls are related by a quasi-D_2 symmetry in NiBCP-8 and a quasi-C_4 symmetry in ZnBCP-8.

For NiBCP-8, the four couplings between each Soret component (lying along one C_2 axis) and the carbonyls are equivalent. Because the torsion angles between each $\pi-\pi^*$ transition dipole and the two mutually orthogonal Soret components are of opposite sign (Figure 3a), rotational strengths of opposite signs are generated by the exciton mechanism (Figure

2c). By contrast, the μ·m mechanism is rather dominated by the position of the porphyrin, well confined within the *xyz* sector, with respect to the carbonyl planes (Figure 3b), whereas the relative orientation between the two μ and **m** dipoles plays a minor role.

For ZnBCP-8, the four C=O bonds are almost parallel/perpendicular to N−N directions. Thus, for each carbonyl, the couplings with one Soret component will be negligible, and the ones surviving are of the same sign.[29]

G. Comparison of Calculated and Observed CD. Inspection of the calculated contributions to the rotational strength for NiBCP-8 and ZnBCP-8 (Figure 2) obviously indicates that
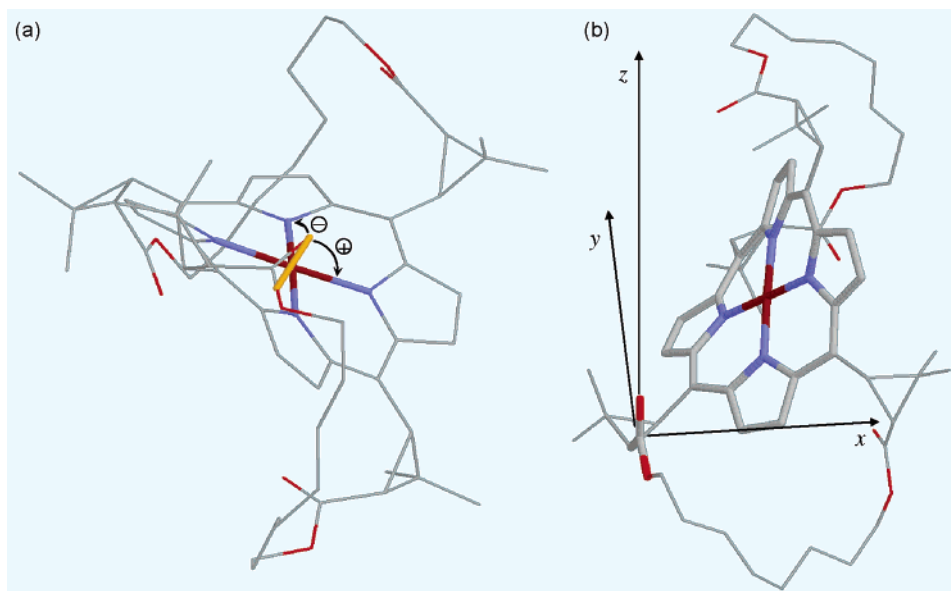
Figure 3. Geometric arrangement between an ester group and the porphyrin ring in the X-ray structure of NiBCP-8. (a) Chiralities defined by the ester $\pi-\pi*$ transition dipole (orange) and the two Soret transition dipoles. (b) Position of the porphyrin ring in the framework useful for the calculation in eq 8: the $n-\pi*$ magnetic transition dipole is oriented along z, and the carboxylate lies in the yz plane. The situation for the other ester groups is roughly equivalent.

an interpretation of the observed CD spectra based on a single mechanism would be erroneous. In the following, individual contributions for each compound are examined, and their respective magnitudes, as reflected in the experimental spectra, are discussed.

The situation is rather clear-cut for $\alpha\alpha\alpha\alpha$-ZnBCP-8, for which a positive Cotton effect is observed. Here, the contributions from inherent chirality (Figure 2b) and the $\mu\cdot m$ with carbonyl $n-\pi*$ (Figure 2f) are of the same positive sign and seem to overcome, by a small amount, the negative signal due to the exciton coupling with the ester $\pi-\pi*$ (Figure 2d). The one-electron mechanism should be of minor importance, because for the C_2-symmetric complex, the perturbations of the two straps (or, better, of the two half-moieties of each strap) tend to cancel each other. Therefore, the observed and calculated CD are in good agreement, and we conclude that the positive Cotton effect of $\alpha\alpha\alpha\alpha$-ZnBCP-8 is mainly associated with the chiral conformation of the porphyrin chromophore. Similar considerations should hold for the free-base $\alpha\alpha\alpha\alpha$-H$_2$BCP-8.

The situation is more complex for $\alpha\beta\alpha\beta$-NiBCP-8. The magnetic-electric coupling between the Soret bands and the $n-\pi*$ carbonyl transitions brings about a moderately intense negative CD (Figure 2e) that is similar to the observed signal, suggesting that it is the main contribution to the CD of NiBCP-8. In contrast, the calculated rotational strength due to intrinsic chirality is a strong bisignate contribution with a prevailing positive lobe (Figure 2a), and the weak contribution from the coupled dipoles mechanism is positive (Figure 2c); both are opposite to the observed Cotton effect, which is negative. These observations suggest that possible inaccuracies in the computed intrinsic contribution should be considered. First, given the proximity between the two Soret transitions, and the uncertainty associated with calculated transition frequencies, the computed energy sequence for the two Soret bands may easily be inaccurate. For example, in the case of semiempirical calculations on carbonmonoxy myoglobin, fluctuations in the relative energy of the two B components were observed for the molecular dynamics-generated heme conformations.[31] Thus, it

is possible that for NiBCP-8, the actual intrinsic CD appears as a positive couplet (i.e., opposite to that shown in Figure 2a). Second, given the close similarity between the chiral D_2 and nonchiral D_{2d} core structures of NiBCP-8 noted above, the calculated intrinsic chirality contributions are probably overestimated. In addition, more or less allowed porphyrin ring fluctuations may further reduce the intrinsic contribution, which practically may be vanishingly small. Thus, we conclude that the negative Cotton effect of $\alpha\beta\alpha\beta$-NiBCP-8 is mainly associated with the magnetic-electric coupling between the Soret bands and the $n-\pi*$ carbonyl transitions; the small long-wavelength positive component, visible for H$_2$BCP-9 and ZnBCP-9 (Figure 1), is instead possibly due to an intrinsic chirality contribution.

Finally, it is worth noting that in the current situation where the three discussed mechanisms tend to balance each other, the fourth possible source of optical activity, namely the one-electron, could in principle play a significant role. For the D_2-symmetric NiBCP-8, the static perturbation exerted by the aliphatic skeleton on the porphyrin transitions is of the same sign for two symmetric half-moieties of each strap, as well as for the two straps themselves. Therefore, the dipole fields exerted by the substituents of the meso groups, in particular the four ester moieties, will provide an overall nonnegligible perturbation potential to one-electron terms[29] involving Soret transitions, the most significant of which likely arises from their mixing with magnetic dipole-allowed low-lying d–d transitions of Ni. Evaluation of this term would require, among others, parameters describing transitions between excited states (namely, transition charge monopoles)[29] that are not available from the computational package employed and whose accuracy would be hard to check anyway. Moreover, the mixing between porphyrin Soret and Ni d–d transitions is directly allowed in the inherently chiral D_2 group; therefore, it is evaluated de facto in the computation of the intrinsic rotational strength. Among the various configurations contributing to the Soret-type transitions, porphyrin π and $\pi*$ Kohn–Sham orbitals (from HOMO−1 to LUMO+1) display apparent contributions from Ni d orbitals, which give rise to Ni-localized magnetic transition

dipoles collinear to the electric transition dipoles localized on the porphyrin. Their combination will therefore generate non-vanishing rotational strengths, which are already included in the values shown in Table 4. It is unlikely that this direct mixing would be significantly altered by the external perturbation due to the substituents.

Conclusion

New insights into the stereochemistry of the BCP-8 complexes have been obtained by DFT calculations. The BCP-8 moiety in the $\alpha\alpha\alpha\alpha$ conformation exhibits a dome-shaped porphyrin that slightly contracts and becomes strongly ruffled upon the $\alpha\alpha\alpha\alpha \rightarrow \alpha\beta\alpha\beta$ isomerization so as to accommodate the alternating up, down meso substituents. The extent to which the porphyrin macrocycle contracts (and stabilizes the $\alpha\beta\alpha\beta$ conformation) or expands (and stabilizes the $\alpha\alpha\alpha\alpha$ conformation) is determined by the occupancy of the stereochemically active $d_{x^2-y^2}$ orbital level, and the constraints imposed by the short bridles play a key role in the accompanying large conformation changes.

Semiempirical and time-dependent DFT calculations disclose a complex origin for the chiroptical properties of NiBCP-8 and ZnBCP-8, in which an intrinsically chiral porphyrin is embedded in a chiral, multichromophoric environment, similar to the situation found in hemoproteins. The CD spectra seem to arise from several competitive mechanisms of optical activity, with no one starkly prevailing, and any simple analysis in terms of only one mechanism would not be justified. Although complete explicit CD calculations on the bridled chiroporphyrins would be possible, at least with semiempirical methods, because suitable geometries are available, it appears that analytical evaluations such as those presented in the present investigation, although approximate, bring deeper insights into the chiroptical properties of these complex and intriguing molecules.

CD spectroscopy is a good reporter of conformation for the bridled chiroporphyrins and their metal complexes. The correlation found between the sign of the CD signal in the Soret region and the conformation of the BCP-8 compounds is a significant result that may have important operational value: simple inspection of CD spectra might allow a facile determination of the solution conformation of a paramagnetic MBCP-8 compound, for which NMR spectroscopy is uninformative. The conformations of a wide range of MBCP-8 complexes have been examined recently by CD spectroscopy in our laboratories, and the redox-dependent switching of MnClBCP-8 has been observed. Detailed results will be reported in a forthcoming manuscript.

Supporting Information Available: Experimental conditions for acquisition of spectral data. Detailed CD and UV−visible spectra of MBCP-n (M = H_2, Ni, Cu, Zn; n = 8, 9). Complete ref 12. This material is available free of charge via the Internet at http://pubs.acs.org.

JA054926O